

Dissecting Heterogeneous Molecular Chaperone Complexes Using a Mass Spectrum Deconvolution Approach

Florian Stengel,^{1,6,8} Andrew J. Baldwin,^{2,8} Matthew F. Bush,^{1,7} Gillian R. Hilton,¹ Hadi Lioe,¹ Eman Basha,^{3,4} Nomalie Jaya,⁴ Elizabeth Vierling,⁵ and Justin L.P. Benesch^{1,*}

¹Physical and Theoretical Chemistry Laboratory, Department of Chemistry, University of Oxford, Oxford OX1 3QZ, UK

²Departments of Molecular Genetics, Biochemistry, and Chemistry, University of Toronto, Toronto, Ontario M5S 1A1, Canada

³Botany Department, Faculty of Science, Tanta University, Tanta, Gharbia 31111, Egypt

⁴Department of Biochemistry and Molecular Biophysics, University of Arizona, Tucson, AZ 85721, USA

⁵Department of Biochemistry and Molecular Biology, University of Massachusetts, Amherst, MA 01003, USA

⁶Present address: Institute of Molecular Systems Biology, ETH Zürich, CH-8093 Zürich, Switzerland

⁷Present address: Department of Chemistry, University of Washington, Seattle, WA 98195, USA

⁸These authors contributed equally to this work

*Correspondence: justin.benesch@chem.ox.ac.uk

DOI 10.1016/j.chembiol.2012.04.007

SUMMARY

Small heat-shock proteins (sHSPs) are molecular chaperones that prevent irreversible aggregation through binding nonnative target proteins. Due to their heterogeneity, these sHSP:target complexes remain poorly understood. We present a nanoelectrospray mass spectrometry analysis algorithm for estimating the distribution of stoichiometries comprising a polydisperse ensemble of oligomers. We thus elucidate the organization of complexes formed between sHSPs and different target proteins. We find that binding is mass dependent, with the resultant complexes reflecting the native quaternary architecture of the target, indicating that protection happens early in the denaturation. Our data therefore explain the apparent paradox of how variable complex morphologies result from the generic mechanism of protection afforded by sHSPs. Our approach is applicable to a range of polydisperse proteins and provides a means for the automated and accurate interpretation of mass spectra derived from heterogeneous protein assemblies.

INTRODUCTION

Small heat-shock proteins (sHSPs) are a widespread family of molecular chaperones that diverged early in evolution (Waters et al., 1996), with most organisms having multiple sHSP genes (Kappé et al., 2002; Kriehuber et al., 2010). They act as modulators of diverse biological processes, including cytoskeletal dynamics, cell differentiation, aging, and apoptosis (Arrigo and Müller, 2002). In general, their expression is dramatically upregulated during stress conditions (Beck et al., 2009; Malmström et al., 2009), enabling them to form an integral part of the proteo-

stasis network (Balch et al., 2008). As a result, aberrant sHSP function is implicated in a number of diseases including cataracts, cancer, myopathies, motor neuropathies, and neurodegeneration (Arrigo et al., 2007; Carra et al., 2011; Clark and Muchowski, 2000; Dierick et al., 2005; Quinlan and Van Den Ijssel, 1999; Sun and MacRae, 2005).

The current model for sHSP chaperone function is that they are highly dynamic oligomeric structures that exist in an equilibrium between low- and high-target affinity forms (Basha et al., 2012; Haslbeck et al., 2005; Hilton et al., 2012; McHaourab et al., 2009). In vertebrate sHSPs this transition between an active and an inactive state may be regulated by posttranslational modification but in many organisms is mediated by a thermally controlled structural change (Basha et al., 2012; Haslbeck et al., 2005; Hilton et al., 2012; McHaourab et al., 2009). The molecular nature of activation has been variously assigned to dissociation into suboligomeric species (Haslbeck et al., 1999), a conformational switch in the tertiary structure of the protein (Franzmann et al., 2008), or an increase in quaternary dynamics leading to the establishment of a plastic polydisperse ensemble (Stengel et al., 2010). What is clear, however, is that active sHSPs associate with nonnative target proteins, in a reproducible manner, to form stable, soluble complexes, thereby preventing irreversible protein aggregation (Basha et al., 2012; Haslbeck et al., 2005; Hilton et al., 2012; McHaourab et al., 2009). Release and refolding of the target can then occur upon cooperation with ATP-dependent members of the chaperone family, namely HSP70, HSP40, and HSP100 (Cashikar et al., 2005; Lee et al., 1997; Mogk et al., 2003).

Unlike the specific stoichiometries of interaction with target observed for most molecular chaperones (Bukau et al., 2006; Hartl et al., 2011; Saibil, 2008), sHSP:target complexes have proven particularly challenging systems for structural biology, primarily due to their polydispersity (Haley et al., 2000; Stengel et al., 2010). This is further complicated by the sHSPs having broad target specificity (Basha et al., 2004) and the resultant complexes apparently exhibiting variable morphologies (Stromer et al., 2003). In addition, the complexes themselves

appear to be dynamic, capable of the incorporation or exchange of sHSP subunits (Friedrich et al., 2004), and disordered regions of the sHSP are proposed to present diverse geometries of interaction sites (Jaya et al., 2009). As such, insights into the organization and architecture of sHSP:target complexes have proven very difficult to obtain by using traditional techniques.

In the past few years, direct nanoelectrospray mass spectrometry (nanoES MS) analysis of protein assemblies has emerged as a structural biology approach of remarkably general applicability (Heck, 2008; Morgner and Robinson, 2012a; Wyttenbach and Bowers, 2007). Crucially, the effective mass resolution of nanoES MS is very high, enabling not only accurate mass measurement of oligomeric proteins but also the identification of the individual stoichiometries comprising a polydisperse ensemble (Benesch and Ruotolo, 2011). Furthermore, the mass spectra can be used to directly quantify the relative abundance of different oligomers and thereby provide an accurate view of their underlying distribution of stoichiometries (Benesch and Ruotolo, 2011).

In many cases, deconvolution of the MS spectra is achieved using tandem-MS, in which a subset of the protein assemblies are interrogated individually in the gas phase (Benesch, 2009). In the context of this work, such an approach has enabled the identification and relative quantification of the oligomers populated by polydisperse sHSPs (Aquilina et al., 2003; Baldwin et al., 2011b; Benesch et al., 2010a). By employing this tandem-MS strategy, we recently succeeded in determining the gross organization of the complexes formed between a sHSP and a model target (Stengel et al., 2010). We found these complexes to be formed of a variable number of both sHSP and target subunits and showed that this polydispersity arises as a direct result of the thermally controlled quaternary dynamics of the sHSP.

Here, we develop a more detailed and general understanding of sHSP:target complex formation and organization. We examine the interaction of HSP18.1 from pea with three thermolabile targets that differ in mass and quaternary organization: luciferase (Luc; a 60.7 kDa monomer), malate dehydrogenase (MDH; a 71.2 kDa dimer), and citrate synthase (CS; a 103.2 kDa dimer) by means of nanoES MS. We formulate and employ an original automated mass spectrum analysis algorithm, based on optimizing a small number of parameters, to obtain the oligomeric distribution of different sHSP:target complexes. Our approach allows us to elucidate a clear mass dependence of protection and to determine that the nature of the target influences the stoichiometry of the resultant complexes. We find that the native quaternary structure of the targets is at least partially retained, suggesting that binding to HSP18.1 occurs early during their denaturation and providing an explanation as to how the identity of the target can dictate alternative morphologies of the complexes.

RESULTS

NanoES MS Analysis of sHSP:Target Complexes Mirrors In Vitro Measurements

HSP18.1 is a class I sHSP found in the cytosol of pea and is capable of efficiently preventing the irreversible aggregation of thermolabile target proteins (Lee et al., 1995, 1997). Figure 1A

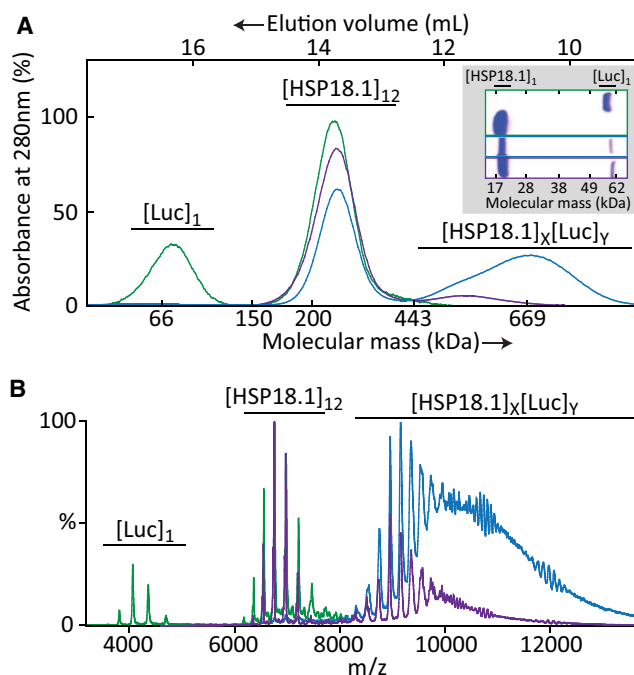


Figure 1. Intact sHSP:Target Complexes Are Amenable to MS Analysis

(A) The SEC trace for HSP18.1 and Luc, in the absence of incubation at heat shock temperatures (green) show two peaks, confirmed by SDS-PAGE (inset) as the individual components. After incubation at 42°C for 10 min, at a ratio (sHSP dodecamer:Luc monomer) of 1:0.1 (purple) or 1:1 (blue) leads to the appearance of an additional broad peak at short elution times. This peak contains both HSP18.1 and Luc, as demonstrated by SDS-PAGE (inset, lanes colored as in the main figure).

(B) Corresponding nESI MS spectra, colored as in (A), mirror the SEC data, with the heat-treated sample revealing additional signal at high mass, corresponding to sHSP:target complexes.

shows size-exclusion chromatography (SEC) traces, performed at 4°C, of different incubations of HSP18.1 and Luc. Without heating (green), two distinct peaks are observed at approximately 16.3 ml and 13.7 ml, which, after calibration, we can assign to monomeric Luc and dodecameric HSP18.1, respectively. Incubation of a 1:0.1 molar ratio of sHSP and Luc (dodecamer:monomer) at 45°C for 10 min (purple) shows the complete disappearance of the peak corresponding to free Luc, a decrease in the peak corresponding to HSP18.1 dodecamer, and the appearance of a broad feature centered near 11.7 ml. SDS-PAGE of this new peak reveals the presence of both HSP18.1 and Luc, indicating the formation of sHSP:target complexes (inset). An identical incubation, but at a 1:1 ratio (blue), shows the formation of more complex and a concomitant further decrease in the HSP18.1 dodecamer. At this higher ratio of target to sHSP, the peak corresponding to complex is notable for its breadth, spanning from 9 to 13 ml, and a mass range of 400 to >1,300 kDa. This demonstrates a significant degree of polydispersity in the sHSP:target complexes. Such heterogeneous complexes are formed reproducibly and reliably, in agreement with previous data obtained for this sHSP (Friedrich et al., 2004).

As the resolution of SEC is limited and does not enable the separation of the different species comprising such

heterogeneous ensembles, we analyzed the complexes formed by means of nanoES MS. Figure 1B shows mass spectra obtained from the different incubations; in the case of the heated samples, the abundance of complex was enhanced by examining pooled fractions eluting after 13 ml (Figure 1A). Prior to heating, two charge state series are observed around 4,000 m/z and 6,500 m/z corresponding to free Luc monomer and HSP18.1 dodecamer, respectively (green). In concord with the SEC experiments, after incubation at 45°C and quenching on ice, the signal for free Luc disappears and is replaced by a broad region of signal at above 8,000 m/z . The relative intensity of this new signal is amplified as the ratio of sHSP to target is changed from 1:0.1 (purple) to 1:1 (blue), which, by comparison to the SEC data, indicates that it arises from sHSP:target complexes. The appearance of the high m/z region of the spectrum is not typical for that expected from a small number of discrete ion populations but rather is characteristic of a polydisperse ensemble (Aquilina et al., 2003; Smith et al., 2006). This mirrors the SEC data and demonstrates not only that HSP18.1 can form a wide range of complexes with targets, thus preventing thermally induced precipitation, but also that the ensemble can be transferred into the gas phase for interrogation by means of nanoES MS (Stengel et al., 2010).

Comparing Calculated and Experimental NanoES Spectra Reveals the Distribution of Polydisperse sHSP:Target Ensembles

While such sHSP:target complexes can be maintained intact in the gas phase, the extensive congestion in the spectra arising from the multitude of oligomeric states renders conventional analysis of the mass spectra challenging. As such, we had previously developed a tandem-MS approach, which capitalizes on the charge-reducing effect of collision-induced dissociation, to allow identification of the different underlying species (Benesch et al., 2006). Combining multiple tandem MS spectra enables the reconstruction of the distribution of polydisperse ensembles (Stengel et al., 2010). Here we chose to develop and apply an alternative strategy, implemented in an algorithm called CHAMP (Calculating Heterogeneous Assembly and Mass Spectra of Proteins), based upon comparing calculated and experimental mass spectra.

In overview, using only empirical relationships obtained for protein assemblies in the gas phase, our approach converts a candidate distribution of sHSP:target stoichiometries into a theoretical nanoES spectrum (for a detailed description, see [Experimental Procedures](#) and [Supplemental Information](#) available online). Multiple such candidate distributions are automatically generated, and their corresponding spectra modeled using starting parameters independent of the experimental data. Our strategy therefore differs from other spectrum deconvolution approaches (Aquilina et al., 2003; Morgner and Robinson, 2012b; Sobott et al., 2002a; van Breukelen et al., 2006). Furthermore, by relying on the objective minimization of a χ^2 function, is unbiased by the user.

In order to test our approach, we used CHAMP to interpret the nanoES mass spectrum obtained for HSP18.1:Luc complexes, formed at a ratio of 1:0.1, as shown in Figure 1. We chose this ratio as it provides complete protection of the target protein (Friedrich et al., 2004) while still allowing us to address all formed

complexes in a single MS experiment, as previously described (Stengel et al., 2010). By varying the candidate distribution of complexes and assessing the correspondence between the calculated spectrum and experimental data, CHAMP returned an excellent best fit (Figure 2A), with an average error of 1.2% (see [Supplemental Information](#)). This clearly enabled us to accurately identify and quantify the different components of the polydisperse ensemble of sHSP:target complexes (Figure 2A, colored lines in insets). A number of stoichiometries are present to an appreciable abundance, with the most populated state being [HSP18.1]₁₈[Luc]₁. Indeed, the vast majority of the complexes contain a single Luc subunit, with a significant population containing two Luc subunits also present (Figure 2B).

To cross-validate our approach, we compared the results obtained by using CHAMP to those determined from tandem-MS experiments. Specifically, we extracted the contribution of different oligomers to the peaks at 8,950 and 9,150 m/z in the best fitting calculated spectrum. This was then compared to experimentally derived distributions for the same two peaks obtained by means of tandem-MS. It is notable how the distributions obtained from the two different approaches both showed a distinctive “saw-tooth” pattern, with complexes containing an even number of subunits outweighing those comprised of an odd number (Figure 2C). This reflects a native dimeric substructure in complexes formed by HSP18.1 (Stengel et al., 2010), though the presence of oligomers comprising an odd number of sHSP subunits indicates the dimer interface to nonetheless be relatively labile (Cheng et al., 2008; Sobott et al., 2002a). Furthermore, the overall distributions obtained from the two independent approaches are comparable, with the calculated data centered on 18.5 ± 0.6 subunits of HSP18.1 bound to a single Luc and the tandem-MS data centered on 19.4 ± 0.4 . The slight difference in centroid values can be rationalized by the enhanced collisional activation of higher charge state ions (Benesch et al., 2009) resulting in their modest overrepresentation in the tandem-MS data. As such, CHAMP represents a reliable means for elucidating the stoichiometries populated, revealing both gross and detailed features of the underlying distributions.

sHSP:Target Complex Distributions Are Variable and Have a Global Organization Dependent on Target Mass

Thus validated, we applied our approach to analyze complexes formed between HSP18.1 and three different targets, Luc, MDH, and CS. These model targets were chosen as their thermally induced destabilization and protection from aggregation by interaction with sHSPs has been extensively studied (Basha et al., 2012), and they span a range of monomer masses and chain lengths (Luc, 60.7 kDa, 550 residues; CS, 51.6 kDa, 464 residues; and MDH, 35.6 kDa, 338 residues). Complexes were formed between HSP18.1 and each target at incubation ratios of 1:0.1 and 1:1 (dodecamer:monomer), isolated by means of SEC, and examined by nanoES MS (Figure 3A, black spectra). The experimental data are in very good agreement with their corresponding best fit simulations obtained using CHAMP (colors), with average errors below 2.6% in all cases. It is possible to display the theoretical spectra of individual subpopulations of components. Examination of the spectra for all sHSP stoichiometries bound to different numbers of MDH subunits, i.e., each

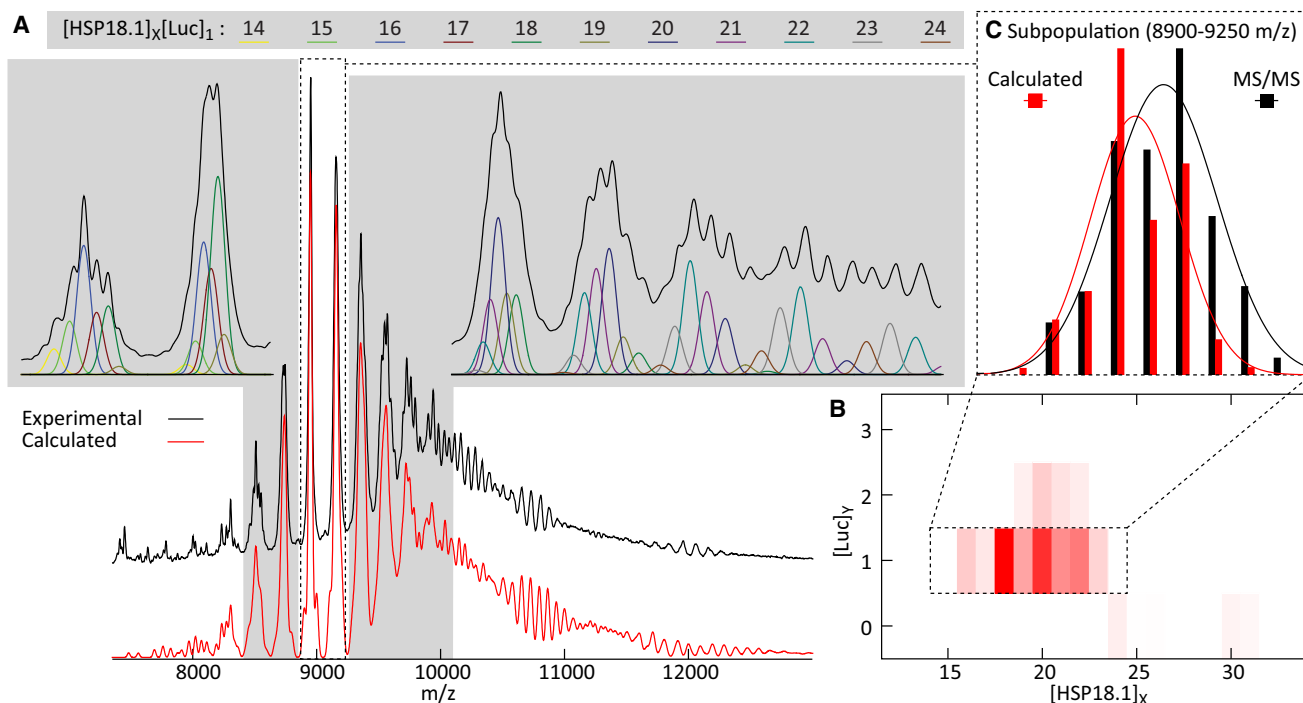


Figure 2. Fitting Simulated Mass Spectra to Experimental Data

(A) Experimental nanoES mass spectrum of HSP18.1:Luc complex formed at a ratio of 1:0.1 dodecamer:monomer (black), overlaid with the best-fitting simulated mass spectrum obtained by using CHAMP in free mode (red). Inset are expansions of regions demonstrating the quality of the fit between experimental and simulated data and the contribution of the different individual HSP18.1:Luc stoichiometries. Our approach is able to identify the species comprising the polydisperse ensemble and their relative intensity.

(B) Distribution map of the relative abundances of all stoichiometries, which gives the spectrum shown in (A).

(C) Comparison of the different complexes contributing to the peaks at 8,950 and 9,150 m/z obtained using CHAMP (red) and by means of tandem-MS (black). The two approaches correlate very well, validating CHAMP as a useful means for estimating the oligomers comprising polydisperse ensembles.

See also Figure S1.

one-dimensional skewed Gaussian in the “set” fit (Figure S1), allows the contribution of that particular MDH “state” to the overall mass spectrum to be assessed and displayed (Figure 3B). It is noticeable how the mean m/z increases as a function of number of MDH subunits even though no restriction is placed on how the individual “bound states” relate to each other. This is intuitively expected and provides further validation of our approach for the deconvolution of polydisperse ensembles.

Having obtained good approximations of the experimental data using CHAMP, we can analyze the likely distributions of oligomers in the context of our knowledge of the native forms of the targets (Figure 4). It is clear that a wide range of sHSP:target stoichiometries are possible: In the case of MDH, over 100 stoichiometries are detected to be populated over 5% of the most abundant. Furthermore, complexes containing in excess of 40 sHSP subunits are detected. This corroborates our previous studies on HSP18.1 and Luc (Stengel et al., 2010) and reveals a remarkable heterogeneity of the complexes.

Increasing the concentration of target protein is reflected in the distributions typically shifting toward complexes containing more subunits of each component (Figure 4A). It is clear, however, that despite the equivalent molar incubation ratio between sHSP and different targets, the resulting complex distributions are very different. To assess the effect of target mass on

the resultant complexes, we plotted the average number of target molecules bound per oligomer as a function of the target monomer mass (Figure 4B). There is a clear negative correlation, demonstrating that the larger the target, the fewer copies thereof can be protected by a given oligomer. This suggests that the sHSP binding capacity is limited by the total mass of client. Plotting the average number of sHSPs in complexes formed at a ratio of 1:0.1 relative to those formed at a ratio of 1:1 reveals a positive correlation with target mass (Figure 4C). This demonstrates that the larger the target, the more sHSPs are required to protect an increased burden of nonnative protein (Basha et al., 2012).

sHSP Complexes Reflect the Native Quaternary Organization of the Target

The target proteins we investigated were chosen because they differ not only in molecular weight but also in quaternary organization. Luc natively exists as a monomer (Conti et al., 1996), whereas CS (Larson et al., 2009) and MDH (Gleason et al., 1994) exist in solution as dimers. It is interesting to note that, at a ratio of 1:0.1, the majority of complexes between HSP18.1 and Luc, natively a monomer, are those with only one target bound, whereas the picture that emerges for the native dimers MDH and CS is clearly different. In these cases, the majority of complexes are those between the sHSP and two target proteins.

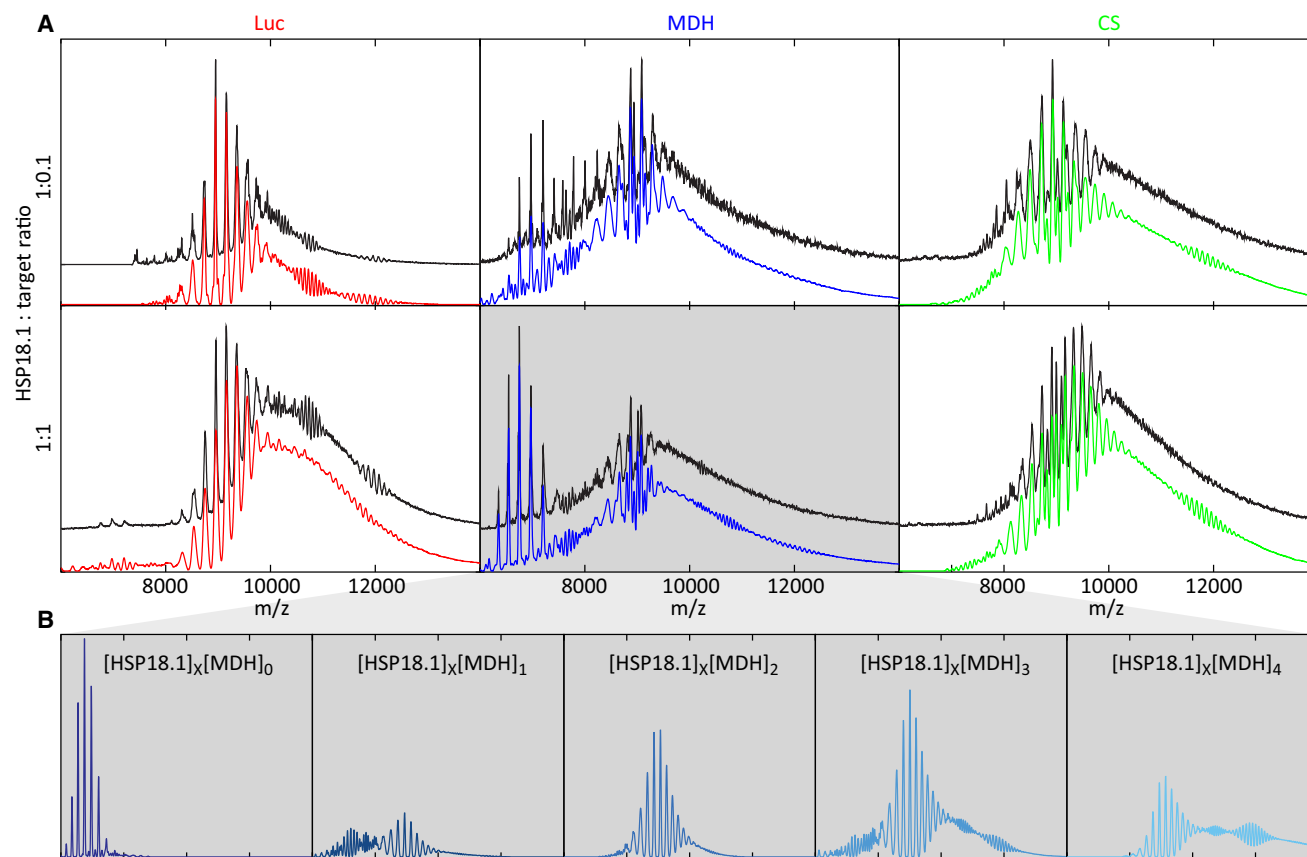


Figure 3. Complexes Formed with sHSPs Exhibit Target-Specific Variability

(A) Experimental (black) and best-fitting calculated (red) spectra of the 200–600 kDa SEC fraction, at incubation ratios of 1:0.1 (upper panel) and 1:1 (lower panel) of HSP18.1 with target (Luc, red; MDH, blue; and CS, green). In all cases, the best fit as determined by CHAMP, operating in set mode, matches the experimental data very well (error ~2%).

(B) Modeled mass spectra for the separate target protein stoichiometries for the 1:1 incubation with MDH reveal a clear increase in m/z with increasing numbers of bound target. This intuitive result provides further validation of the CHAMP fits. The x-axis for the spectra in (B) is identical to that in (A).

Moreover, CHAMP allows us to quantify the relative amount of sHSP:target complexes containing a single target versus those containing two. The ratios of [target]₁: [target]₂ were found to be 2.2:1, 1:1.9, and 1:2.0 for Luc, MDH, and CS, respectively. At the higher incubation ratio of target and sHSP (Figure 4A, lower row), the equivalent values were 1:1.1, 1:1.6, and 1:2.9 for Luc, MDH, and CS, respectively, reflecting the increase in average mass upon the addition of more sHSP. Notably, however, this analysis shows that, in the case of targets that are dimers in the native state, MDH and CS, a significantly higher amount of complexes contain two targets than in the case of the native monomer Luc.

Furthermore, it is notable that the preference for binding dimers appears more pronounced for CS than it is for MDH. This is in line with the areas of the respective dimer interfaces, with that in CS (4,306 Å²) approaching three times that of MDH (1,522 Å²), as calculated from Protein Data Base (PDB) files 3ENJ (Larson et al., 2009) and 1MLD (Gleason et al., 1994), respectively, using the European Bioinformatics Institute service PISA (Krissinel and Henrick, 2007). This might be indicative of HSP18.1 binding MDH concomitant to the dissociation of the

dimer. Combined, our data thus reveal that the preferred sHSP binding pattern is governed to large extent by the mass of the target in question and, at least to a certain degree, also reflects the native conformation of the target.

DISCUSSION

We have investigated the interaction between HSP18.1 from pea with different model target proteins by combining an MS strategy with a mass spectrum analysis approach. This strategy is based on our theoretical and empirical understanding of protein complexes in the gas phase and allows accurate modeling of the spectra arising from polydisperse protein ensembles. By fitting the calculated spectra to the experimental data, we can extract the likely distribution of the sHSP:target complexes formed by HSP18.1 with different targets. This has enabled us to obtain unique and detailed insights into the determinants of the formation of these complexes between chaperone and target and the resulting architecture.

We find that the average number of sHSP subunits within a complex scales with target mass. This can be rationalized by

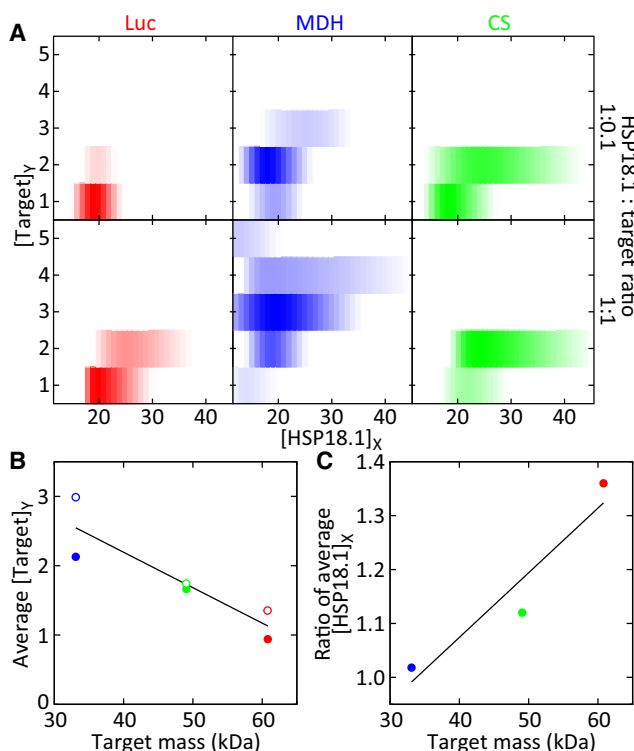


Figure 4. Target-Binding Pattern Reflects the Mass and Organization of the Target

(A) Best fitting distributions of complexes corresponding to the spectra in Figure 3, at incubation ratios of 1:0.1 (upper panel) and 1:1 (lower panel) of HSP18.1 with target (Luc, red; MDH, blue; and CS, green). Comparison between the different targets reveals clear differences, with the native dimeric state of MDH and CS reflected in the distributions. Furthermore, comparison of complexes formed at different sHSP:target ratios demonstrates not only target-specific distributions but also that they “grow” differently, consistent with different targets leading to different complex morphologies.

(B) Protection by HSP18.1 correlates with target protein mass. A plot of the average number of target proteins per complex versus the monomeric mass of the target reveals a clear negative correlation. Colors are as in (A), with solid and empty circles representing 1:0.1 and 1:1 ratios, respectively.

(C) Plotting the average number of sHSP subunits within the complexes formed at a ratio 1:1, divided by that at a ratio of 1:0.1, demonstrates a positive scaling with target mass.

See also Figure S2.

considering that the number of nonpolar residues in a protein is loosely dependent on its sequence length. Therefore, by extension, we would expect the amount of hydrophobic surface exposed during denaturation to approximately scale with molecular mass. It is interesting that, for all targets examined, we observed significant abundances only of complexes containing more sHSP subunits than in the “native” dodecamer, suggesting that sHSP:target complexes are based on higher order sHSP oligomers. This is in line with our previous results in which we demonstrated that, at elevated temperatures, HSP18.1 subunits are reversibly redistributed into a range of oligomeric states (Stengel et al., 2010) and provides further evidence that the dodecamer represents an inactive storage form.

Little is known about the kinetic details of the protection conferred by sHSPs. Indeed, both early and late unfolding inter-

mediates of the target have been identified as binding structures (Carver et al., 2002; Lee et al., 1997; Lindner et al., 2001). Difficulties arise in studying the unfolding intermediates as these target states are extremely aggregation prone in isolation (Cheng et al., 2008). We reason that, if the target were to be bound by the sHSP at an early time point of its unfolding process, aspects of its native structure should be retained. Our data show that, in the case of the native homodimers MDH and CS, a significantly higher amount of sHSP:target complexes containing two target subunits are found than in the case of the native monomer Luc. The composition of sHSP:target complexes seems therefore to be influenced by the oligomerization of the target itself, consistent with HSP18.1 protecting targets early in the denaturation process.

If the target is protected early during unfolding, it will necessarily retain considerable native structural characteristics rather than being unstructured. This mirrors findings from hydrogen/deuterium exchange MS measurements, which revealed the conformation of MDH in complex with HSP18.1 to retain considerable core structure (Cheng et al., 2008). Furthermore, these findings provide a rationale for previous observations of variable sHSP:target complex morphologies (Stromer et al., 2003). As such, we expect the morphology of sHSP:target complexes to not only vary with the identity of target but also to reflect its underlying architecture.

Previous work has suggested that the sHSPs form a dynamic and plastic ensemble of species (Basha et al., 2012; Haslbeck et al., 2005; Hilton et al., 2012; McHaourab et al., 2009) as part of the overall chaperone network of the cell (Gong et al., 2009). In this way, the sHSPs can protect a wide variety of target proteins and therefore form a crucial part of the cellular proteostasis machinery (Balch et al., 2008). We have investigated the interaction between HSP18.1 from pea with different model target proteins by combining an MS strategy with a novel mass spectrum analysis approach. Our results demonstrate that target protection benefits not only from the diversity of this sHSP subnetwork but also from the rapid action of these chaperones. The picture that emerges is one of an sHSP network of broad specificity, mediated by the quaternary dynamics of the sHSP oligomer, which can respond rapidly to bind targets early during their unfolding under cellular stress.

SIGNIFICANCE

We have presented a means of interpreting mass spectra and applied it to polydisperse ensembles formed between sHSPs and their targets. Over the past two decades, both mass spectrometry (MS) instrumentation and experimental methodologies for structural biology have undergone considerable advances (Hilton and Benesch, 2012). The development of approaches for interpreting the resulting nanoelectrospray (nanoES) spectra has, however, been underexplored, and data analysis remains largely performed manually. Aside from the bias this may introduce, it currently represents a major bottleneck in the MS analysis of protein assemblies. The objective nature of CHAMP circumvents these difficulties and is, therefore, well suited to the automated analysis of the mass spectra of protein assemblies. Such approaches will be significant not only for the

quantitative interpretation of nanoES data for the extraction of thermodynamic and kinetic parameters (Baldwin et al., 2011b; Ebong et al., 2011) but also for the goal of high-throughput MS-based structural biology.

While the development of CHAMP has enabled us to glean insights into the molecular chaperone function of sHSPs, it is directly applicable to the analysis of other molecules similarly complicated by polydispersity. This property renders many proteins and self-assembling molecules refractory to structural characterization, as most methods provide an average overall species in solution. In contrast, the inherently “separative” nature of MS can be exploited to allow the structural interrogation of individual proteins within a mixture. This can be performed either in the gas phase by means of ion-mobility spectrometry (Baldwin et al., 2011a; Pukala et al., 2009; Smith et al., 2010) or by deposition for ex situ electron microscopy analysis (Benesch et al., 2010b). The approach described here will further strengthen the role of MS in the study of heterogeneous proteins, particularly when integrated with other structural techniques that report at higher structural resolution (Robinson et al., 2007).

EXPERIMENTAL PROCEDURES

Protein Preparation

HSP18.1 from *Pisum sativum* (pea) was expressed in *Escherichia coli* and purified as described previously (Lee et al., 1995). Recombinant firefly Luc was purchased from Promega (Catalog No. E1701), mitochondrial pig heart MDH was purchased from Roche Applied Sciences (Catalog No. 10127256001), and pig heart CS was purchased from Sigma Aldrich (Catalog No. C3260-200UN). All samples were exchanged into the buffer of choice using SEC on a Superdex 200 HR10/300 column (GE Healthcare) or a centrifugal concentrator (5K MWCO Vivaspın, Sartorius) and adjusted to the desired concentration using theoretical extinction coefficients (Pace et al., 1995).

Complex Formation

The particular target protein was incubated with a final concentration of 12 μM HSP18.1 (dodecamer) at the desired molar ratio in 150 mM KCl, 5 mM MgCl_2 , 2 mM HEPES, 2 mM DTT, pH 7.5, at 45°C. The incubation time for Luc was 10 min, and for MDH and CS it was 60 min, after which the reaction was quenched on ice. This was followed by SEC into 200 mM ammonium acetate, pH 6.8, using a Superdex 200 HR10/300 column (GE Healthcare) kept at 4°C. Denaturing SDS-PAGE of the different SEC fractions was performed using precast gels and the SeeBlue Plus 2 marker (both Invitrogen).

Prior to MS analysis, the desired SEC fractions were concentrated using centrifugal concentrators (5K MWCO Vivaspın, Sartorius) to a final concentration of $\sim 2 \mu\text{M}$. For the 1:1 sHSP:target ratios, we concentrated only the 200–600 kDa SEC fraction, as these species are amenable to MS analysis and allowed us to investigate the initial stages of complex formation.

NanoES MS Analysis

Mass spectra were obtained on a quadrupole time-of-flight (Q-ToF) mass spectrometer (Q-ToF 2, Waters, Milford MA, USA) modified for high-mass operation (Sobott et al., 2002b), using a previously described protocol (Hernández and Robinson, 2007). Relevant instrument parameters are the following: nanoES capillary, 1,600 V; sample cone, 160 V; extractor cone, 40 V; ion transfer stage, 1.0×10^{-2} mbar; quadrupole analyzer, 1.0×10^{-5} mbar; and ToF analyzer, 8.1×10^{-6} mbar. The collision cell was held at 35 μbar argon, and an accelerating voltage of 30 V and 200 V applied for MS and tandem-MS experiments, respectively. Spectra were calibrated externally using a 33 mg/ml aqueous solution of cesium iodide (Sigma). Data were acquired and processed with MassLynx software (Waters, Milford MA, USA) and are shown with minimal smoothing.

Calculation of Theoretical Mass Spectra

Calculated spectra were generated automatically using an algorithm coded in C++ that is based in principle on two previously described approaches (Sobott et al., 2002a; van Breukelen et al., 2006). CHAMP takes an input distribution of species comprising multiple components, e.g., sHSP and target subunits, and generates a predicted nanoES mass spectrum using empirical relationships derived from the literature and additional experiments. The full model is detailed in the Supplemental Information, but, briefly, a given theoretical mass spectrum is calculated from a candidate distribution as follows.

Each complex is assumed to give rise to a Gaussian distribution of charge states in the gas phase, where the sum of all the ions is proportional to the total concentration of the complex in the solution phase. The centroid of the distribution is based on the empirical relationship between mass and average charge state, $Z_A = 0.0467 m^{0.533}$ (Stengel et al., 2010) and is offset by a variable, F (constant for each spectrum), that accounts for charge-state variations between different nanoES capillaries (Li and Cole, 2003).

The m/z value of each charge state is adjusted by a parameter, Q , which scales according to the surface area of the protein complex, to take into account the adduction of ions and molecules from the buffer (McKay et al., 2006). The peak width is optimized according to a resolution factor, R , which accommodates the m/z dependence of peak width (McKay et al., 2006) and accounts for the differences in effective resolution between different nanoES spectra (Keetch et al., 2003). The intensity of the peak is scaled to account for the m/z dependence of detector sensitivity (Fraser, 2002), the primary determinant of variations in response for nanoES experiments of molecules at high m/z (Chen et al., 2003).

By repeating this process for all individual species within our sHSP:target distribution, a simulated nanoES mass spectrum can be generated for any distribution of complexes as a function of just three physical parameters, F , Q , and R , which collectively act to address small variations in the spectra that result from differences in the mass spectra due to the nanoES spray conditions (Hernández and Robinson, 2007). The parameters that were held constant during the calculation of candidate spectra presented here, were the following: $M_P = 17,985$ Da (mass of HSP18.1); $M_P = 60,803$ Da (Luc), 33,100 Da (MDH), and 49,072 Da (CS); $Z_W = 1.4$ (from measurements of four different dodecameric sHSPs), $A_O = 60$, and $V_A = 9.1$ kV (the detector “open area” and ToF accelerating voltage, respectively, both instrument-specific constants; see Supplemental Information). For any given distribution of complexes, the parameters F , Q , and R were varied freely until the best fit between calculated and experimental spectra was obtained.

Fitting of Theoretical Mass Spectra to Experimental Results

In order to obtain a view of the distribution underlying a nanoES mass spectrum, CHAMP varies the candidate distribution to find the lowest χ^2 between a calculated spectrum and experimental data. A direct “steepest descent” minimization of all the free parameters was found to frequently get trapped in different local minima of relatively high χ^2 , depending on the initial conditions. Consequently, a more sophisticated strategy was employed to ensure that the minimizer can get as close to the global lowest χ^2 as possible. The algorithm uses a sequential three-stage fitting procedure, and we refer to the ensuing best fit distributions as the surface, set, and free fits for Stages 1–3, respectively (Figure S1).

In the first stage, in order to reduce the number of free parameters that specify the sHSP:target distribution, it is approximated by a two-dimensional Gaussian-like function that is free to skew in the sHSP dimension. This distribution was found to be of sufficient complexity that reasonably good fits to all the data sets in the study were obtained but is still specified by a relatively small number of parameters. With reference to Figure S1, the five parameters that specify this surface fit are: the most probable sHSP stoichiometry (a), the most probable target stoichiometry (b), the width in both the sHSP and target dimensions (a_w and b_w , respectively), and the degree of skewness in the sHSP dimension (α). To best approach the global minimum, a trial distribution of the two centroid parameters (a and b) and the remaining parameters (a_w , b_w , and α) is minimized according to a Levenberg-Marquardt steepest descent algorithm. This procedure is repeated for a range of centroid positions so that we can determine the χ^2 as a function of these two parameters. In this way, the globally lowest χ^2 for this model can be robustly approached.

To further refine the best fitting distribution, a second level of complexity can be applied. Starting from the distribution refined from the surface fit, the distribution for each given target stoichiometry ($b_i, i = 0, 1, 2, \dots, j$) is assumed to be independent and specified by a three-parameter skewed Gaussian function (Figure S1). The number of free parameters correspondingly increases to three times the number of stoichiometries b_i considered and results in the set fit. An F test is performed at this stage to ensure that the reduction in χ^2 from going to a more complex model by including these additional free parameters is statistically justified.

In the third and final stage, taking the set fit as the starting point, the abundance of each individual complex is considered a free parameter, which is minimized to further lower the χ^2 . This free fit represents the highest resolution implementation of CHAMP. The validation of its use is similarly assessed using an F test and, in the data presented here, was justified for the spectra in Figure 2.

SUPPLEMENTAL INFORMATION

Supplemental Information includes two figures and Supplemental Experimental Procedures and can be found with this article online at doi:10.1016/j.chembiol.2012.04.007.

ACKNOWLEDGMENTS

We thank Nina Morgner (University of Oxford) for critical review of the manuscript, and acknowledge funding from the European Union 7th Framework Program "PROSPECTS" (F.S.), the Canadian Institutes of Health Research (A.J.B.), Waters UK Ltd. (M.F.B.), the Wellcome Trust (F.S. and G.R.H.), the European Molecular Biology Organization (A.J.B. and H.L.), the National Institutes of Health Grant GM42762 (N.J., E.B., and E.V.), and the Royal Society (J.L.P.B.).

Received: December 21, 2011

Revised: April 2, 2012

Accepted: April 6, 2012

Published: May 24, 2012

REFERENCES

- Aquilina, J.A., Benesch, J.L.P., Bateman, O.A., Slingsby, C., and Robinson, C.V. (2003). Polydispersity of a mammalian chaperone: mass spectrometry reveals the population of oligomers in alphaB-crystallin. *Proc. Natl. Acad. Sci. USA* *100*, 10611–10616.
- Arrigo, A.-P., and Müller, W.E.G., eds. (2002). *Small stress proteins (Progress in molecular and subcellular biology)* (New York: Springer).
- Arrigo, A.P., Simon, S., Gibert, B., Kretz-Remy, C., Nivon, M., Czekalla, A., Guillet, D., Moulin, M., Diaz-Latoud, C., and Vicart, P. (2007). Hsp27 (HspB1) and alphaB-crystallin (HspB5) as therapeutic targets. *FEBS Lett.* *581*, 3665–3674.
- Balch, W.E., Morimoto, R.I., Dillin, A., and Kelly, J.W. (2008). Adapting proteostasis for disease intervention. *Science* *319*, 916–919.
- Baldwin, A.J., Lioe, H., Hilton, G.R., Baker, L.A., Rubinstein, J.L., Kay, L.E., and Benesch, J.L.P. (2011a). The polydispersity of α B-crystallin is rationalized by an interconverting polyhedral architecture. *Structure* *19*, 1855–1863.
- Baldwin, A.J., Lioe, H., Robinson, C.V., Kay, L.E., and Benesch, J.L.P. (2011b). α B-crystallin polydispersity is a consequence of unbiased quaternary dynamics. *J. Mol. Biol.* *413*, 297–309.
- Basha, E., Lee, G.J., Brechi, L.A., Hausrath, A.C., Buan, N.R., Giese, K.C., and Vierling, E. (2004). The identity of proteins associated with a small heat shock protein during heat stress in vivo indicates that these chaperones protect a wide range of cellular functions. *J. Biol. Chem.* *279*, 7566–7575.
- Basha, E., O'Neill, H.O., and Vierling, E. (2012). Small heat shock proteins and α -crystallins: dynamic proteins with flexible functions. *Trends Biochem. Sci.* *37*, 106–117.
- Beck, M., Malmström, J.A., Lange, V., Schmidt, A., Deutsch, E.W., and Aebersold, R. (2009). Visual proteomics of the human pathogen *Leptospira interrogans*. *Nat. Methods* *6*, 817–823.
- Benesch, J.L.P. (2009). Collisional activation of protein complexes: picking up the pieces. *J. Am. Soc. Mass Spectrom.* *20*, 341–348.
- Benesch, J.L.P., and Ruotolo, B.T. (2011). Mass spectrometry: come of age for structural and dynamical biology. *Curr. Opin. Struct. Biol.* *21*, 641–649.
- Benesch, J.L.P., Aquilina, J.A., Ruotolo, B.T., Sobott, F., and Robinson, C.V. (2006). Tandem mass spectrometry reveals the quaternary organization of macromolecular assemblies. *Chem. Biol.* *13*, 597–605.
- Benesch, J.L.P., Ruotolo, B.T., Sobott, F., Wildgoose, J., Gilbert, A., Bateman, R., and Robinson, C.V. (2009). Quadrupole-time-of-flight mass spectrometer modified for higher-energy dissociation reduces protein assemblies to peptide fragments. *Anal. Chem.* *81*, 1270–1274.
- Benesch, J.L.P., Aquilina, J.A., Baldwin, A.J., Rekas, A., Stengel, F., Lindner, R.A., Basha, E., Devlin, G.L., Horwitz, J., Vierling, E., et al. (2010a). The quaternary organization and dynamics of the molecular chaperone HSP26 are thermally regulated. *Chem. Biol.* *17*, 1008–1017.
- Benesch, J.L.P., Ruotolo, B.T., Simmons, D.A., Barrera, N.P., Morgner, N., Wang, L., Saibil, H.R., and Robinson, C.V. (2010b). Separating and visualising protein assemblies by means of preparative mass spectrometry and microscopy. *J. Struct. Biol.* *172*, 161–168.
- Bukau, B., Weissman, J., and Horwich, A. (2006). Molecular chaperones and protein quality control. *Cell* *125*, 443–451.
- Carra, S., Crippa, V., Rusmini, P., Boncoraglio, A., Minoia, M., Giorgetti, E., Kampinga, H.H., and Poletti, A. (2011). Alteration of protein folding and degradation in motor neuron diseases: Implications and protective functions of small heat shock proteins. *Prog. Neurobiol.* *10.1016/j.pbr.2011.1003.1031*.
- Carver, J.A., Lindner, R.A., Lyon, C., Canet, D., Hernandez, H., Dobson, C.M., and Redfield, C. (2002). The interaction of the molecular chaperone α -crystallin with unfolding α -lactalbumin: a structural and kinetic spectroscopic study. *J. Mol. Biol.* *318*, 815–827.
- Cashikar, A.G., Duennwald, M., and Lindquist, S.L. (2005). A chaperone pathway in protein disaggregation. Hsp26 alters the nature of protein aggregates to facilitate reactivation by Hsp104. *J. Biol. Chem.* *280*, 23869–23875.
- Chen, X., Westphall, M.S., and Smith, L.M. (2003). Mass spectrometric analysis of DNA mixtures: instrumental effects responsible for decreased sensitivity with increasing mass. *Anal. Chem.* *75*, 5944–5952.
- Cheng, G., Basha, E., Wysocki, V.H., and Vierling, E. (2008). Insights into small heat shock protein and substrate structure during chaperone action derived from hydrogen/deuterium exchange and mass spectrometry. *J. Biol. Chem.* *283*, 26634–26642.
- Clark, J.I., and Muchowski, P.J. (2000). Small heat-shock proteins and their potential role in human disease. *Curr. Opin. Struct. Biol.* *10*, 52–59.
- Conti, E., Franks, N.P., and Brick, P. (1996). Crystal structure of firefly luciferase throws light on a superfamily of adenylate-forming enzymes. *Structure* *4*, 287–298.
- Dierick, I., Irobi, J., De Jonghe, P., and Timmerman, V. (2005). Small heat shock proteins in inherited peripheral neuropathies. *Ann. Med.* *37*, 413–422.
- Ebong, I.O., Morgner, N., Zhou, M., Saraiva, M.A., Daturpalli, S., Jackson, S.E., and Robinson, C.V. (2011). Heterogeneity and dynamics in the assembly of the heat shock protein 90 chaperone complexes. *Proc. Natl. Acad. Sci. USA* *108*, 17939–17944.
- Franzmann, T.M., Menhorn, P., Walter, S., and Buchner, J. (2008). Activation of the chaperone Hsp26 is controlled by the rearrangement of its thermosensor domain. *Mol. Cell* *29*, 207–216.
- Fraser, G.W. (2002). The ion detection efficiency of microchannel plates (MCPs). *Int. J. Mass Spectrom.* *215*, 13–30.
- Friedrich, K.L., Giese, K.C., Buan, N.R., and Vierling, E. (2004). Interactions between small heat shock protein subunits and substrate in small heat shock protein-substrate complexes. *J. Biol. Chem.* *279*, 1080–1089.
- Gleason, W.B., Fu, Z., Birktoft, J., and Banaszak, L. (1994). Refined crystal structure of mitochondrial malate dehydrogenase from porcine heart and the

- consensus structure for dicarboxylic acid oxidoreductases. *Biochemistry* 33, 2078–2088.
- Gong, Y., Kakihara, Y., Krogan, N., Greenblatt, J., Emili, A., Zhang, Z., and Houry, W.A. (2009). An atlas of chaperone-protein interactions in *Saccharomyces cerevisiae*: implications to protein folding pathways in the cell. *Mol. Syst. Biol.* 5, 275.
- Haley, D.A., Bova, M.P., Huang, Q.L., Mchaourab, H.S., and Stewart, P.L. (2000). Small heat-shock protein structures reveal a continuum from symmetric to variable assemblies. *J. Mol. Biol.* 298, 261–272.
- Hartl, F.U., Bracher, A., and Hayer-Hartl, M. (2011). Molecular chaperones in protein folding and proteostasis. *Nature* 475, 324–332.
- Haslbeck, M., Walke, S., Stromer, T., Ehrnsperger, M., White, H.E., Chen, S., Saibil, H.R., and Buchner, J. (1999). Hsp26: a temperature-regulated chaperone. *EMBO J.* 18, 6744–6751.
- Haslbeck, M., Franzmann, T., Weinfurter, D., and Buchner, J. (2005). Some like it hot: the structure and function of small heat-shock proteins. *Nat. Struct. Mol. Biol.* 12, 842–846.
- Heck, A.J. (2008). Native mass spectrometry: a bridge between interactomics and structural biology. *Nat. Methods* 5, 927–933.
- Hernández, H., and Robinson, C.V. (2007). Determining the stoichiometry and interactions of macromolecular assemblies from mass spectrometry. *Nat. Protoc.* 2, 715–726.
- Hilton, G.R., and Benesch, J.L.P. (2012). Two decades of studying non-covalent biomolecular assemblies by means of electrospray ionization mass spectrometry. *J. R. Soc. Interface* 9, 801–816.
- Hilton, G.R., Lioe, H., Stengel, F., Baldwin, A.J., and Benesch, J.L.P. (2012). Small heat-shock Proteins: paramedics of the cell. *Top. Curr. Chem.*, in press.
- Jaya, N., Garcia, V., and Vierling, E. (2009). Substrate binding site flexibility of the small heat shock protein molecular chaperones. *Proc. Natl. Acad. Sci. USA* 106, 15604–15609.
- Kappé, G., Leunissen, J.A., and de Jong, W.W. (2002). Evolution and diversity of prokaryotic small heat shock proteins. *Prog. Mol. Subcell. Biol.* 28, 1–17.
- Keetch, C.A., Hernández, H., Sterling, A., Baumert, M., Allen, M.H., and Robinson, C.V. (2003). Use of a microchip device coupled with mass spectrometry for ligand screening of a multi-protein target. *Anal. Chem.* 75, 4937–4941.
- Kriehuber, T., Rattei, T., Weinmaier, T., Bepperling, A., Haslbeck, M., and Buchner, J. (2010). Independent evolution of the core domain and its flanking sequences in small heat shock proteins. *FASEB J.* 24, 3633–3642.
- Krissinel, E., and Henrick, K. (2007). Inference of macromolecular assemblies from crystalline state. *J. Mol. Biol.* 372, 774–797.
- Larson, S.B., Day, J.S., Nguyen, C., Cudney, R., and McPherson, A. (2009). Structure of pig heart citrate synthase at 1.78 Å resolution. *Acta Crystallogr. Sect. F Struct. Biol. Cryst. Commun.* 65, 430–434.
- Lee, G.J., Pokala, N., and Vierling, E. (1995). Structure and in vitro molecular chaperone activity of cytosolic small heat shock proteins from pea. *J. Biol. Chem.* 270, 10432–10438.
- Lee, G.J., Roseman, A.M., Saibil, H.R., and Vierling, E. (1997). A small heat shock protein stably binds heat-denatured model substrates and can maintain a substrate in a folding-competent state. *EMBO J.* 16, 659–671.
- Li, Y., and Cole, R.B. (2003). Shifts in peptide and protein charge state distributions with varying spray tip orifice diameter in nano-electrospray Fourier transform ion cyclotron resonance mass spectrometry. *Anal. Chem.* 75, 5739–5746.
- Lindner, R.A., Treweek, T.M., and Carver, J.A. (2001). The molecular chaperone α -crystallin is in kinetic competition with aggregation to stabilize a monomeric molten-globule form of α -lactalbumin. *Biochem. J.* 354, 79–87.
- Malmström, J., Beck, M., Schmidt, A., Lange, V., Deutsch, E.W., and Aebersold, R. (2009). Proteome-wide cellular protein concentrations of the human pathogen *Leptospira interrogans*. *Nature* 460, 762–765.
- McHaourab, H.S., Godar, J.A., and Stewart, P.L. (2009). Structure and mechanism of protein stability sensors: chaperone activity of small heat shock proteins. *Biochemistry* 48, 3828–3837.
- McKay, A.R., Ruotolo, B.T., Ilag, L.L., and Robinson, C.V. (2006). Mass measurements of increased accuracy resolve heterogeneous populations of intact ribosomes. *J. Am. Chem. Soc.* 128, 11433–11442.
- Mogk, A., Schlieker, C., Friedrich, K.L., Schönfeld, H.J., Vierling, E., and Bukau, B. (2003). Refolding of substrates bound to small Hsps relies on a disaggregation reaction mediated most efficiently by ClpB/DnaK. *J. Biol. Chem.* 278, 31033–31042.
- Morgner, N., and Robinson, C.V. (2012a). Linking structural change with functional regulation—insights from mass spectrometry. *Curr. Opin. Struct. Biol.* 22, 44–51.
- Morgner, N., and Robinson, C.V. (2012b). Massign: an assignment strategy for maximizing information from the mass spectra of heterogeneous protein assemblies. *Anal. Chem.* 84, 2939–2948.
- Pace, C.N., Vajdos, F., Fee, L., Grimsley, G., and Gray, T. (1995). How to measure and predict the molar absorption coefficient of a protein. *Protein Sci.* 4, 2411–2423.
- Pukala, T.L., Ruotolo, B.T., Zhou, M., Politis, A., Stefanescu, R., Leary, J.A., and Robinson, C.V. (2009). Subunit architecture of multiprotein assemblies determined using restraints from gas-phase measurements. *Structure* 17, 1235–1243.
- Quinlan, R., and Van Den Ijssel, P. (1999). Fatal attraction: when chaperone turns harlot. *Nat. Med.* 5, 25–26.
- Robinson, C.V., Sali, A., and Baumeister, W. (2007). The molecular sociology of the cell. *Nature* 450, 973–982.
- Saibil, H.R. (2008). Chaperone machines in action. *Curr. Opin. Struct. Biol.* 18, 35–42.
- Smith, A.M., Jahn, T.R., Ashcroft, A.E., and Radford, S.E. (2006). Direct observation of oligomeric species formed in the early stages of amyloid fibril formation using electrospray ionisation mass spectrometry. *J. Mol. Biol.* 364, 9–19.
- Smith, D.P., Radford, S.E., and Ashcroft, A.E. (2010). Elongated oligomers in β 2-microglobulin amyloid assembly revealed by ion mobility spectrometry-mass spectrometry. *Proc. Natl. Acad. Sci. USA* 107, 6794–6798.
- Sobott, F., Benesch, J.L.P., Vierling, E., and Robinson, C.V. (2002a). Subunit exchange of multimeric protein complexes. Real-time monitoring of subunit exchange between small heat shock proteins by using electrospray mass spectrometry. *J. Biol. Chem.* 277, 38921–38929.
- Sobott, F., Hernández, H., McCammon, M.G., Tito, M.A., and Robinson, C.V. (2002b). A tandem mass spectrometer for improved transmission and analysis of large macromolecular assemblies. *Anal. Chem.* 74, 1402–1407.
- Stengel, F., Baldwin, A.J., Painter, A.J., Jaya, N., Basha, E., Kay, L.E., Vierling, E., Robinson, C.V., and Benesch, J.L.P. (2010). Quaternary dynamics and plasticity underlie small heat shock protein chaperone function. *Proc. Natl. Acad. Sci. USA* 107, 2007–2012.
- Stromer, T., Ehrnsperger, M., Gaestel, M., and Buchner, J. (2003). Analysis of the interaction of small heat shock proteins with unfolding proteins. *J. Biol. Chem.* 278, 18015–18021.
- Sun, Y., and MacRae, T.H. (2005). The small heat shock proteins and their role in human disease. *FEBS J.* 272, 2613–2627.
- van Breukelen, B., Barendregt, A., Heck, A.J., and van den Heuvel, R.H. (2006). Resolving stoichiometries and oligomeric states of glutamate synthase protein complexes with curve fitting and simulation of electrospray mass spectra. *Rapid Commun. Mass Spectrom.* 20, 2490–2496.
- Waters, E.R., Lee, G.J., and Vierling, E. (1996). Evolution, structure and function of the small heat shock proteins in plants. *J. Exp. Bot.* 47, 325–338.
- Wytttenbach, T., and Bowers, M.T. (2007). Intermolecular interactions in biomolecular systems examined by mass spectrometry. *Annu. Rev. Phys. Chem.* 58, 511–533.